

## DISPLACEMENT-BASED SEISMIC DESIGN OF CONCRETE BRIDGES

V.G. Bardakis<sup>1</sup> and M.N. Fardis<sup>2</sup>

<sup>1</sup> Post-Doctoral Researcher, Structures Lab, Dept. of Civil Engineering, University of Patras, Patras, Greece

<sup>2</sup> Professor & Director, Structures Laboratory, Dept. of Civil Engineering, University of Patras, Patras, Greece  
Email: fardis@upatras.gr

### ABSTRACT :

A Displacement-based seismic design procedure is proposed and elaborated for concrete bridges with continuous deck integral with the piers. It includes a simple estimation of inelastic deformation demands (chord or plastic hinge rotations in piers, curvatures for the deck) via elastic 5%-damped modal response spectrum analysis. The applicability of the equal displacement rule at the level of member deformations is checked through nonlinear dynamic analyses of eight representative bridges, regular or irregular, with three or five spans, all with a prestressed concrete box girder and piers of various cross-sections and about equal or very different heights. The procedure gives more cost-effective designs than the conventional force-based approach of Eurocode 8, without loss in seismic performance under ground motions well beyond the design motion.

**KEYWORDS:** Concrete bridges, Displacement-based design, Eurocode 8, Seismic design of bridges

### 1. INTRODUCTION

Recent years have seen displacement-based design (DBD) emerging as the most promising basis for the future developments in seismic design. In this new approach seismic displacements and deformations are the primary response variables for the design; capacity-demand comparisons for ductile members are expressed in terms of them, instead of forces. DBD concepts have advanced more for buildings than for bridges. This paper is an effort to close the gap for concrete bridges with piers integral with a continuous prestressed-concrete deck.

### 2. PROPOSED DISPLACEMENT-BASED SEISMIC DESIGN PROCEDURE

The proposed procedure consists of several steps:

**Step 1:** Dimensioning of the deck and the piers for:

- the Ultimate Limit State (ULS) under the combination of factored permanent and traffic loads at all relevant intermediate stages of construction and in the completed bridge configuration, taking into account the redistribution of action effects due to creep and loss of prestressing, etc., as appropriate;
- the Serviceability Limit State (SLS) under the pertinent combinations of permanent and transient actions in the completed bridge.

**Step 2:** Estimation of an effective stiffness of the piers and the (almost finally dimensioned in Step 1) deck,  $(EI)_{\text{eff}}$ , representative of their elastic stiffness during the seismic response (longitudinal or transverse) :

- For bending of the deck about the horizontal axis (about which the section and prestressing are normally asymmetric),  $(EI)_{\text{eff}}$  is taken from a moment-curvature ( $M-\varphi$ ) diagram as the secant stiffness between: (a) the point of cracking (decompression, for zero concrete tensile strength) under bending that induces tension in the mean tendon, and (b) the point of first yielding of reinforcement in the opposite direction of bending.
- For deck bending about the vertical axis  $(EI)_{\text{eff}}$  is taken as 85% of the elastic stiffness of the uncracked gross concrete section. This value fits well, on average, the first slope of a bilinear fitting of the  $M-\varphi$  diagram.
- For the piers,  $(EI)_{\text{eff}}$  should be the secant stiffness to yielding of those end sections where plastic hinging is expected under the design seismic action and the concurrent gravity loads: at the base of each pier and at its

connection to the deck for the longitudinal seismic action, or at the base of alone for the transverse one. This value depends on the geometry of the section, the moment-to-shear ratio at the end section (“shear span”,  $L_s$ ), the axial load  $N$  and the amount and layout of vertical reinforcement (Biskinis and Fardis, 2006). For Step 2 (i.e., before dimensioning the piers for the seismic action)  $(EI)_{\text{eff}}$  may be estimated from an empirical expression by Biskinis and Fardis (2006) in terms only of the geometry of the section,  $N$  and  $L_s$ .

**Step 3:** Estimation of (elastic or inelastic) deformations (chord rotations,  $\theta_{\text{Ed}}$ , at pier ends, deck curvatures,  $\varphi_{\text{Ed}}$ ) for the two horizontal components of the design earthquake via 5%-damped modal response spectrum analysis.

**Step 4:** Selection of a target value of the chord rotation ductility factor,  $\mu_\theta$ , at pier ends where plastic hinges are expected under the design seismic action and estimation of the target chord rotation at yielding,  $\theta_y$ , there as:

$$\theta_y = \theta_{\text{Ed}} / \mu_\theta \quad (1.1)$$

with  $\theta_{\text{Ed}}$  from Step 3. This gives the opportunity to target a uniform level of inelasticity between piers of different height, etc. Then, the pier yield moment,  $M_y$ , corresponding to the value of  $\theta_y$  from Eq. 1.1 is found as:

$$M_y = 3(EI)_{\text{eff}} \theta_y / L_s \quad (1.2)$$

using the same values of secant stiffness to yielding at the pier end sections,  $(EI)_{\text{eff}}$ , and of the shear span,  $L_s$ , as in Step 2. The pier vertical reinforcement is then dimensioned to provide the yield moment,  $M_y$ , from Eq. 1.2. Note that this step, which is the parallel of dividing internal forces from an elastic analysis with the 5%-damped spectrum analysis by a global behavior factor  $q$  (or response modification factor  $R$ ) in force-based design is not essential. Its objective is to promote uniform distribution of inelasticity and avoid overstrength in the piers. If it turns out that the vertical reinforcement in some piers is governed by Step 1, instead of this step, it is recommended to reduce the target value of  $\mu_\theta$  until Step 4 finally governs then vertical reinforcement in all piers.

**Step 5:** Ensuring that the deck will not yield under the curvature  $\varphi_{\text{Ed}}$  induced by the design seismic action and that due to the concurrent quasi-permanent loads,  $\varphi_{\text{G+}\psi\text{Q+P}}$ :

$$\varphi_{\text{G+}\psi\text{Q+P}} \pm \gamma_o \varphi_{\text{Ed}} \leq \varphi_{\text{yd}} \quad (1.3)$$

where  $\varphi_{\text{yd}}$  is the design value of the deck yield curvature (value at yielding in a  $M-\varphi$  diagram, divided by the partial factor for steel,  $\gamma_s$ ) and  $\gamma_o = 1.35\gamma_s$  an overstrength factor to account for strain-hardening and remove  $\gamma_s$  in the piers. To satisfy Eq. 1.3, it may be necessary to increase the prestressing and/or the reinforcement over the requirements from Step 1, or to increase the size of the piers in order to reduce  $\varphi_{\text{Ed}}$ .

**Step 6:** Verification of the piers for the chord rotation demands from Step 3 for both horizontal components of the design seismic action:

$$\theta_{\text{Ed}} \leq \theta_{\text{Rd}} \quad (1.4)$$

$\theta_{\text{Rd}} = \theta_{\text{uk},0.05} / \gamma_{\text{Rd}}$  is the design value of the pier chord rotation capacity,  $\theta_{\text{uk},0.05}$  is the 5%-fractile of the pier ultimate chord rotation and  $\gamma_{\text{Rd}}$  a resistance factor,  $\gamma_{\text{Rd}}$ . The expression by Biskinis and Fardis (2006) are used for the calculation of the expected value of the pier ultimate chord rotation,  $\theta_{\text{um}}$ , and of  $\theta_{\text{uk},0.05} = 0.5 \theta_{\text{um}}$ . For a design seismic action with 10% probability of exceedance in 50 years, an appropriate value is  $\gamma_{\text{Rd}} = 2$ . The pier confining reinforcement is the main free dimensioning variable governing  $\theta_{\text{um}}$  and should be dimensioned to meet Eq. 1.4.

**Step 7:** Verification (or increase) of the cross-sectional size of the piers in shear and dimensioning of their transverse reinforcement, so that:

- We prevent brittle shear failure before plastic hinging, by dimensioning the full height of the pier so that:

$$V_{CD} \leq V_{Rd,mon} \quad (1.5)$$

- piers can safely sustain the cyclic degradation of shear resistance in the plastic hinge due to the inelastic deformations predicted for the plastic hinge from the analysis in Step 3:

$$V_{CD} \leq V_{Rd,cyc}(\mu_\theta) \quad (1.6)$$

where:

- $V_{CD}$  is the “capacity design” shear force, determined on the basis of equilibrium, assuming that piers develop their overstrength moment capacity,  $\gamma_o M_{Rd}$ , at both top and bottom sections for bending in the longitudinal direction of the bridge, or only at the base for bending in the transverse direction, where  $M_{Rd}$  is the design value of the pier moment capacity and  $\gamma_o$  the overstrength factor above.
- $V_{Rd,cyc}(\mu_\theta)$  is the design value of shear resistance in cyclic loading after flexural yielding from Biskinis et al (2004) and is a decreasing function of the chord rotation ductility factor,  $\mu_\theta$ . Once the pier vertical reinforcement has been dimensioned in Step 4,  $\mu_\theta$  can be taken as  $\theta_{Ed}$  at the pier end section from Step 3 divided by  $\theta_y$ , there, calculated according to Step 7 below;
- $V_{Rd,mon}$ : is the design value of shear resistance for monotonic loading (as for non-seismic actions), equal to  $V_{Rd,cyc}(\mu_\theta=1)$ , with  $V_{Rd,cyc}(\mu_\theta)$  as above.

**Step 8:** Verification (or increase) of the cross-sectional size of the deck in shear and torsion and dimensioning of its transverse reinforcement under the shears and the torque due to the concurrent quasi-permanent loads (collectively denoted as  $E_{G+\psi Q+P}$ ) combined with overstrength shears and torques due to the design seismic action, obtained as their elastic estimates from Step 4 (collectively denoted as  $E_{Ed}$ ) divided by the target pier chord rotation ductility factor,  $\mu_\theta$ , used in Step 4, as:

$$E_d = E_{G+\psi Q+P} \pm \gamma_o E_{Ed} / \mu_\theta \quad (1.7)$$

**Step 9:** Updating of the secant stiffness to yielding at the pier end sections,  $(EI)_{eff}$ , by inverting Eq. 1.2, using there the value of  $\theta_y$  calculated from the expressions in Biskinis and Fardis (2006) on the basis of the amount and layout of the pier vertical reinforcement from Step 4 and of the shear span (moment-to-shear ratio),  $L_s$ , from the elastic analysis of Step 3. If the so-computed values of  $(EI)_{eff}$  deviate significantly from those determined for the piers in Step 2 and used in Step 3 to estimate the deformation demands, then Steps 3 to 8 are repeated, until convergence of the value of  $(EI)_{eff}$  from Step 9 and the effective stiffness used in the analysis.

## 2. NONLINEAR DYNAMIC VS MODAL RESPONSE SPECTRUM ANALYSIS OF BRIDGES

For the estimation of pier inelastic deformation demands via elastic modal response spectrum analysis as proposed for Step 3, the applicability of the “equal displacement” rule to the level of member deformations should be established. This has been pursued by comparing results of nonlinear dynamic and of modal response spectrum analysis for eight representative bridges. A computational capability has been developed for modelling, seismic response analysis and evaluation of concrete bridges and used for this end. The tool is program ANSRuop-bridges ([www.ansruop.net](http://www.ansruop.net)), developed at the University of Patras as a significantly enhanced version of the ANSR-I program of Mondkar and Powel (1975). Analysis capabilities include (but are not limited to):

1. Elastic analysis for any static loads concurrent with the seismic action, where deck tendons are replaced by statically equivalent distributed loads along their length and concentrated forces and moments at deviations or anchorages, for the determination of the initial condition for the seismic analysis of the bridge;
2. 5%-damped elastic seismic analysis: modal response spectrum analysis with CQC and static analysis under transverse or longitudinal lateral forces proportional to nodal masses and response accelerations constant along the deck and inverted triangular up the piers, or from the mode with the largest participating mass in the horizontal direction considered, all at a fundamental period in that direction from the Rayleigh quotient;
3. Nonlinear static (“pushover”) seismic analysis with lateral force patterns as in 2 above;
4. Nonlinear dynamic analysis, under one or two earthquake components (time-histories).

A pre-processor constructs  $M-\phi$  diagrams of any section at the pier or the deck for the initial value of the axial force due to loads acting concurrently with the seismic action and the pre-strains of the tendons. Decompression, cracking, yielding or flexural failure of the section are automatically identified and the secant stiffness to these points determined. The pre-processor computes the shear and torsional rigidity of the section, including or not the effect of cracking (with user-specified fractions of the elastic rigidity of the uncracked gross section). For the piers, the expressions in Biskinis and Fardis (2006) are used for  $M_y$  and  $(EI)_{ef}$  (cf. Eq. 1.2 and discussion in Step 9 above for  $(EI)_{eff}$  and  $\theta_y$ ). For nonlinear analysis, these properties, as well as  $\theta_{um}$  and  $V_{Rd,cyc}(\mu_\theta)$  (cf. Steps 6 and 7 above) are updated during the response depending on the current values of  $N$ ,  $L_s$  and  $\mu_\theta$ .

Deck and piers are discretized longitudinally into a series of prismatic beam elements in 3D, with inelasticity lumped at point hinges at the ends and taken independent and uncoupled in the two transverse directions of bending. Moment-rotation relations at point hinges in the deck, derived from the  $M-\phi$  diagram of the deck section, are multilinear, with corners at section cracking and yielding. All the elements into which a pier is discretised have the same  $(EI)_{eff}$ -value, computed from Eq. 1.2 using there the values of  $M_y$  and  $\theta_y$  from Biskinis and Fardis (2006) at the end sections of the pier where plastic hinging may take place and as  $L_s$  the moment-to-shear-ratio at those end sections: generally half the pier clear height, except for single piers under the transverse component of the seismic action, where the full clear height is used. The effect of the variation of  $N$  during the response and M-N interaction are considered in each direction ( $M_y$ - $N$  and  $M_z$ - $N$ ). P- $\Delta$  effects are included. Joints between the deck and the piers are considered as rigid. Slippage of vertical bars of the pier from the joint or from the foundation is accounted for, by including in the corresponding  $(EI)_{ef}$  value of the pier the effect of the resulting fixed-end rotation of the end sections.

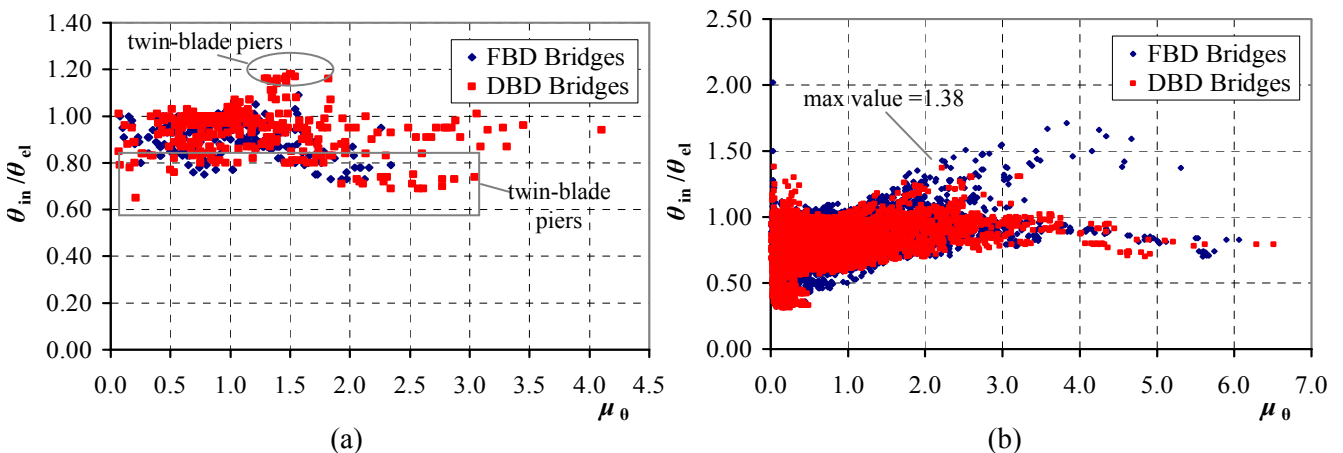


Figure 1: Average ratio of maximum chord rotation demand from nonlinear dynamic analyses to that from elastic time-history analysis for the 7 input motions: (a) at pier ends; (b) at all points where deck is discretised.

To check the applicability of the “equal displacement” rule to the level of member deformations, 8 bridges are subjected to dynamic analyses, linear or nonlinear, separately in the longitudinal or transverse direction) for 7 input motions with PGA on rock 0.25g, 0.35g or 0.45g (times 1.15 on soil top and in addition by an importance factor of 1.3 for 3 of the bridges). All bridges have a prestressed box-girder deck fully restrained transversely at the abutments but free to slide longitudinally. They are variations of two real bridges to produce a representative set of regular or irregular bridges with 3 or 5 spans and piers of circular, hollow rectangular or twin-blade sections with similar or very different heights (Fig. 2). Two versions of each bridge are subjected to comparative nonlinear dynamic and modal response spectrum analyses: one of conventional force-based design according to Eurocode 8 and another designed via the proposed DBD procedure (see Section 3 below). Results are shown in Figure 1 in the form of the ratio of the maximum chord rotation demand over the 7 nonlinear dynamic analyses to 5%-modal response spectrum analysis. They are summarised for all pier ends and all along the deck of the 8 bridges, analysed at 3 PGA levels each separately in the longitudinal or transverse direction. The ratio of inelastic-to-elastic deformations is plotted versus the chord rotation ductility factor,  $\mu_\theta$ , at the element end in question (about 1400 points for piers, about 31000 for the deck). Values of  $\mu_\theta$  less than 1.0 for piers refer to ends

where no plastic hinge forms, e.g., at pier tops for transverse earthquake or (especially for piers of conventional, force-based design) or piers with significant overstrength. Witness that DBD piers exhibit, in general, higher values of  $\mu_\theta$  than those of conventional, force-based design and vice-versa for the deck. As we will see in Section 3, DBD gives a more balanced distribution of inelasticity between piers and deck. As a result, the ratio of inelastic-to-elastic deformations is closer to 1.0, both in the piers and at the deck. Deviations from 1.0 are mostly downwards, especially for the DBD bridges, implying that the elastic estimation of deformations in Step 3 of the proposed DBD procedure is normally safe-sided. All the large deviations for piers (values above 1.15 or below 0.8) are for twin-blade piers in some analyses that neglected the effect of axial load variation on flexural inelasticity (in those cases this effect caused numerical instabilities in the nonlinear analyses). Witness also in Fig. 1(b) that the ascending trend of deviation is limited to decks of conventional force-based design.

### 3. APPLICATION OF PROPOSED DBD PROCEDURE AND EVALUATION OF THE DESIGNS

The proposed DBD procedure was applied for the seismic design of the eight bridges. Fig. 2 compares the amount of pier reinforcement of the DBD bridges to that from force-based design (FBD) of the same bridge. In Fig. 3 the bridge seismic performance is evaluated and compared in terms of the following three measures of response and performance, obtained via nonlinear dynamic analyses in the longitudinal or transverse direction for the 7 input motions with PGA on rock 0.25g, 0.35g or 0.45g:

- The peak value of the chord rotation ductility factor,  $\mu_\theta$ , at an element end;
- The damage ratio in flexure, equal to the maximum ratio of flexural deformation demand to the corresponding capacity during the response. The flexural capacity of piers is their expected ultimate chord rotation,  $\theta_{um}$ , from Biskinis and Fardis (2006) (see Step 6 in Section 1) computed on the basis of the current values of  $N$  and  $L_s$ ; for the deck elements, it is half the element length times the curvature where a tendon yields, or the non-prestressed reinforcement ruptures, or the concrete crushes, all from a  $M-\phi$  diagram.
- The damage ratio in shear, obtained as the maximum ratio of shear force demand to capacity during the response. Shear capacity is the cyclic shear resistance,  $V_{Rd,cyc}(\mu_\theta)$ , at the current value of  $\mu_\theta$  and is estimated according to Biskinis *et al* (2004) (see Step 7 in Section 1) on the basis of the current values of  $N$ ,  $L_s$  and  $\mu_\theta$ .

The piers of the DBD bridges have much lower vertical reinforcement ratio than in the FBD versions. They also have lower (or at most the same) transverse steel ratios. As a result, the pier ductility factor,  $\mu_\theta$ , is in general larger in the DBD than in the FBD bridge, especially in the longitudinal direction, where the relative stiffness and flexural resistance of the deck and the piers make a difference in the seismic response. In the same direction, the deck by contrast, is subjected to much less inelastic action in the DBD version of the bridge than in the FBD one, although is the same. It is clear that DBD gives a more balanced distribution of inelasticity between the piers and the deck and prevents excessive inelastic action in the deck, which is normally not designed for the seismic action and may yield on the side of the section opposite to the one where the tendons are.

It is interesting to note that the DBD piers, despite their lower vertical and transverse reinforcement, have about the same safety margin against failure in flexure or shear as their FBD counterparts. This margin is comfortable, even for seismic actions more than 3-times the design one. Similar to the point made before about the magnitude of their inelastic demands, under longitudinal seismic action the decks of FBD bridges may suffer in flexure, while their DBD counterparts have a significant safety margin. By contrast, the decks of the DBD bridges may sometimes have significantly lower – albeit still ample – safety margins in shear than their FBD counterparts.

Owing to the very little vertical reinforcement in the DBD piers, the pier secant stiffness to yielding is overestimated by the reinforcement-independent empirical expression for  $(EI)_{eff}$  in Biskinis and Fardis (2006), fitted to test data with much higher steel ratios. So, Steps 3-8 were repeated after updating the value of  $(EI)_{eff}$  in Step 9 using the more accurate expressions in Biskinis and Fardis (2006) and the actual pier reinforcement. Table 3.1 shows that the final values of the fundamental periods of the DBD version of the bridge,  $T_L$  and  $T_S$ , are longer than the ones from Steps 2,  $T_{Lo}$  and  $T_{So}$ . Table 3.1 lists also the fundamental periods of the FBD version of the bridge, computed with  $(EI)_{eff}$  values from the more accurate expressions and the FBD pier reinforcement.

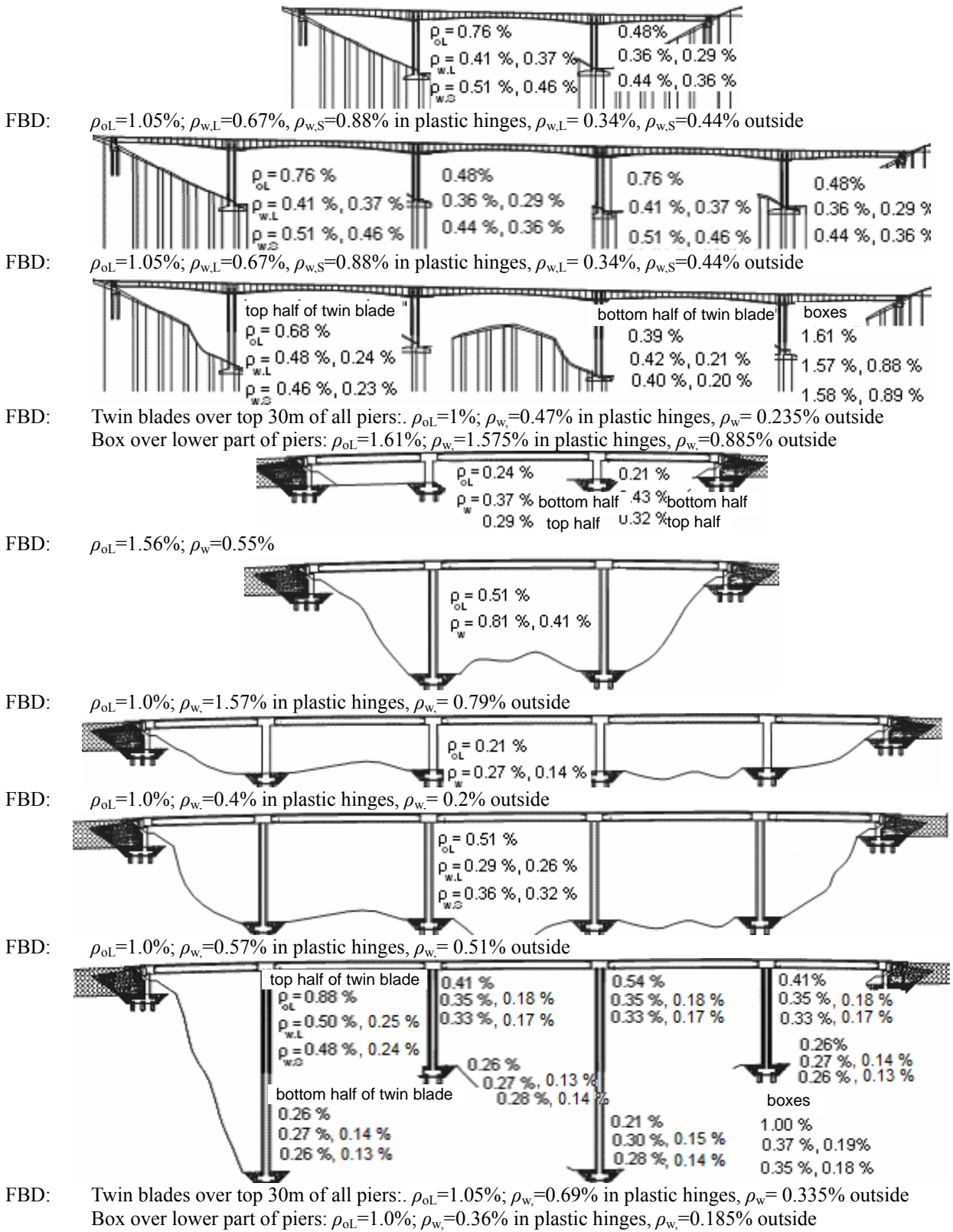


Figure 2: Pier reinforcement ratios in DBD bridges:  $\rho_{OL}$ : vertical,  $\rho_w$ : transverse ( $\rho_{wL}$ ,  $\rho_{wS}$ , if different in bridge longitudinal or transverse direction of rectangular box piers) with 1<sup>st</sup> and 2<sup>nd</sup> value: ratio in or outside plastic hinges. Ratios for force-based design (FBD) are written underneath.

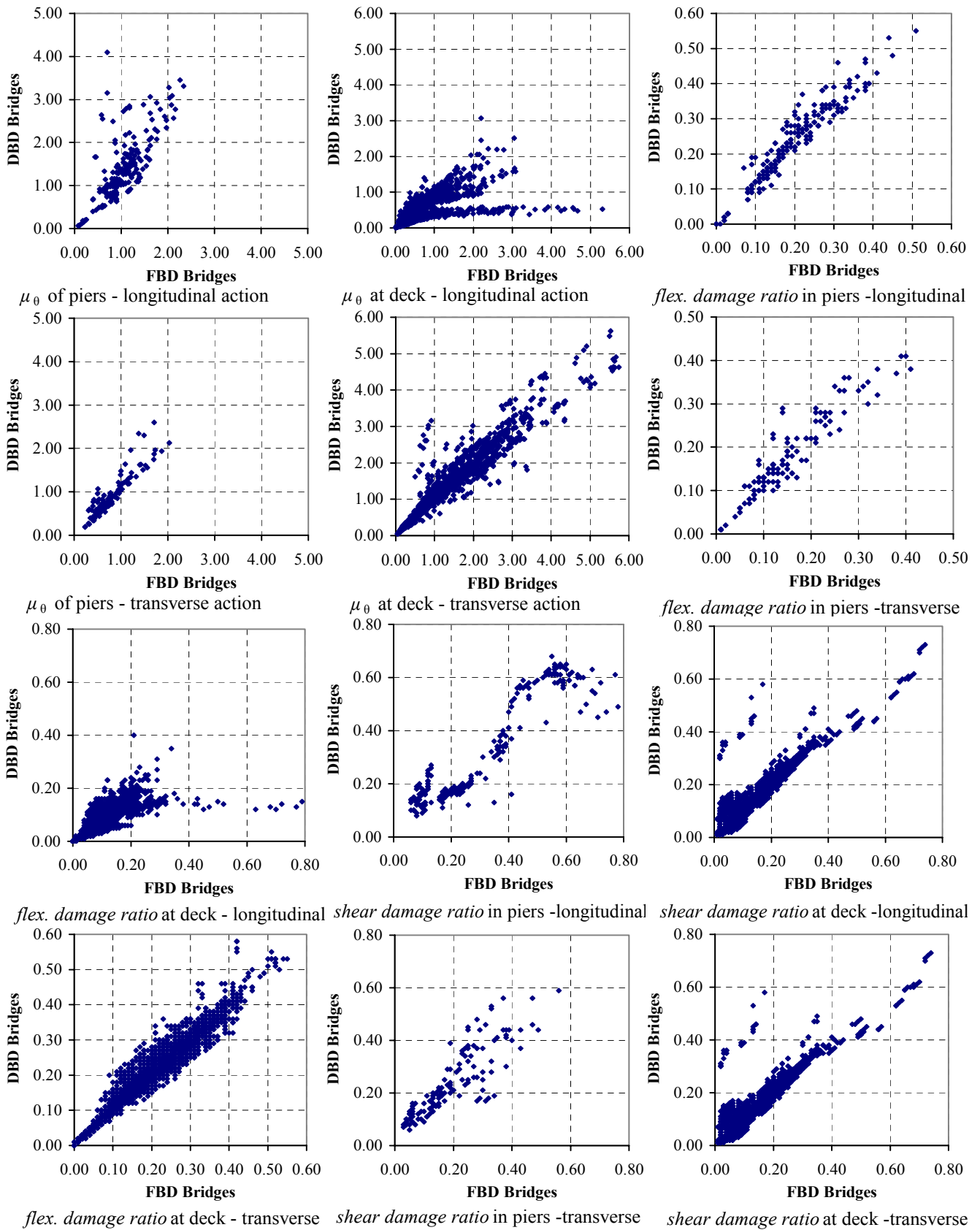


Figure 3: Outcome of nonlinear dynamic analysis (average for 7 motions in each direction) in DBD v force-based bridge designs

Table 3.1: Fundamental periods of the bridge in the longitudinal (L) and the transverse (S) direction, for its FBD and DBD versions ( $T_{Lo}$  and  $T_{So}$ : initial values from Step 2).

Bridge	FBD bridge per EC8		DBD bridge			
	$T_L$ (sec)	$T_S$ (sec)	$T_{Lo}$ (sec)	$T_L$ (sec)	$T_{So}$ (sec)	$T_S$ (sec)
1	2.80	2.72	2.25	2.97	3.03	3.75
2	2.65	4.04	2.18	2.84	3.37	3.71
3	4.64	2.07	4.51	5.36	2.58	2.81
4	0.62	0.86	0.59	0.93	0.83	1.11
5	3.33	1.05	2.59	3.75	1.10	1.13
6	1.47	2.17	1.26	1.86	1.83	2.41
7	1.82	1.91	1.41	2.06	1.55	2.04
8	3.26	2.04	3.03	4.28	2.41	3.17

## 5. CONCLUSIONS

The proposed Displacement-based seismic design procedure for concrete bridges with continuous deck integral with the piers gives more cost-effective and rational designs than the conventional force-based approach, with marked improvements and no substantial loss in seismic performance under ground motions well beyond the design motion. It is based on simple estimation of inelastic deformation demands at pier ends and along the deck via elastic 5%-damped modal response spectrum analysis, presuming that the equal displacement rule may be applied at the level of member deformations. Several hundred nonlinear dynamic analyses of 8 representative bridges, regular or irregular, with three or five spans, with piers of various cross-sections and about equal or similar or very different heights have demonstrated that this rule is overall safe-sided and indeed applicable.

## ACKNOWLEDGEMENT

The support of research project ASPROGE of the Hellenic General Secretariat for Research and Technology and of the European Commission's LESSLOSS project is acknowledged.

## REFERENCES

- Biskinis, D.E. and Fardis, M.N. (2006). Assessment and upgrading of resistance and deformation capacity of RC piers, 1<sup>st</sup> European Conference on Earthquake Engineering and Seismology, Geneva, Paper no.315
- Biskinis, D.E., G.K. Roupakias and Fardis, M.N. (2004). Degradation of shear strength of RC members with inelastic cyclic displacements, *ACI Structural Journal* **101.6**, 773-783
- Mondkar, D.P. and Powel, G.H. (1975). ANSR-I General purpose program for analysis of structural response. Res. Report UCB/EERC 75-37, Earthquake Engineering Research Center, University of California, Berkeley, Ca